Table 1 Values of frequency parameters, $\lambda_f^{1/4}$ of a spring-hinged cantilever beam

γ	λ_J	$\lambda_M = 0.1$	$\lambda_M = 1.0$	$\lambda_M = 10.0$	$\lambda_M = 100.0$
0.01	0.1	0.3700	0.2889	0.1758	0.0998
	1.0	0.2885	0.2556	0.1722	0.0996
	10.0	0.1755	0.1720	0.1487	0.0975
	100.0	0.0996	0.0994	0.0974	0.0839
0.1	0.1	0.6570	0.5121	0.3106	0.1762
	1.0	0.5059	0.4500	0.3040	0.1758
	10.0	0.3058	0.3001	0.2612	0.1720
	100.0	0.1734	0.1731	0.1698	0.1474
1.0	0.1	1.1216	0.8729	0.5202	0.2941
	1.0	0.8009	0.7320	0.5062	0.2933
	10.0	0.4704	0.4647	0.4194	0.2854
	100.0	0.2658	0.2654	0.2622	0.2363
10.0	0.1	1.4679	1.1505	0.6885	0.3895
	1.0	0.9546	0.9003	0.6605	0.3878
	10.0	0.5478	0.5442	0.5116	0.3721
	100.0	0.3087	0.3085	0.3064	0.2880
100.0	0.1	1.5093	1.1924	0.7269	0.4127
	1.0	0.9787	0.9284	0.6940	0.4106
	10.0	0.5599	0.5567	0.5274	0.3917
	100.0	0.3154	0.3152	0.3134	0.2969

of a cantilever beam (for which γ is very large) A, B, and C can be derived from the analysis presented here in by excluding the terms with γ.

Numerical Results

When Eq. (7) derived here is used, the fundamental frequencies of spring-hinged cantilever beams with concentrated mass and rotary inertia at the free end can be evaluated for several cases of interest. The numerical results for the frequency parameter $\lambda_f^{1/4}$ are presented in Table 1 for different values of λ_M, λ_J, and rotational spring stiffness parameter γ. For a cantilever beam with very large values of γ and without concentrated mass and rotary inertia, Eq. (7) yields 1.879 for the frequency parameter, which is in very good agreement (<1% difference) with the published result $\lambda_f^{1/4} = 1.875$) (Ref. 3). The present results given in Table 1, when compared to corresponding results obtained by very accurate finite element method,[4] are in excellent agreement with a four significant figures accuracy for most of the cases. Somewhat less agreement was found for very low values of combined γ, λ_M, and λ_J, where the accuracy is up to three significant figures, even though the difference is less than 1%. The finite element results were compared with results of Lee,[5] and excellent agreement was reported for those presented. The present results are also in excellent agreement with those of Lee, except for a few combinations of γ, λ_J, and λ_M. (For example, for $\gamma = 10$, $\lambda_J = \lambda_M = 0.01$, the difference is about 9.5%, and for $\gamma = 1.0$, $\lambda_J = \lambda_M = 0.01$, the difference is about 5%.) Inasmuchas all other results are in very good agreement, the authors feel the present results are more accurate.

Conclusions

A simple formula for the free vibration behavior of the upper stage of a rocket or missile has been presented. This problem is treated mathematically as a spring-hinged cantilever beam with a concentrated mass and rotary inertia at the free end. The Rayleigh–Ritz method was used to obtain the fundamental frequency from suitably derived admissible functions that represent the spring-hinged boundary condition. Note that the fundamental frequencies obtained in the present study agree very well with those obtained by using a very accurate finite element method. Thus, the present formula can be reliably used to evaluate the fundamental frequency, which is an important design parameter, of a spring-hinged cantilever beam with end concentrated mass and rotary inertia, forming a mathematical model of the upper stage of a rocket/missile. The formula presented should be very useful for design engineers, who need simple, but accurate, closed-form solutions during the design phase.

References

[1]Zienkiewicz, O. C., *The Finite Element Method*, 3rd ed., McGraw–Hill, London, 1977, Chaps. 1–3.

[2]Elishakoff, I., "Apparently First Closed-Form Solution for Frequency of Beam with Rotational Spring," *AIAA Journal*, Vol. 39, No. 1, 2001, pp. 183–186.

[3]Hurty, W. C., and Rubinstein, M. F., *Dynamics of Structures*, Eastern Economy ed., Prentice–Hall of India, New Delhi, India, 1967, p. 203.

[4]Venkateswara Rao, G., and Kanaka Raju, K., "A Galerkin Finite Element Analysis of a Uniform Beam Carrying a Concentrated Mass and Rotary Inertia with a Spring-Hinge," *Journal of Sound and Vibration*, Vol. 37, No. 4, 1974, pp. 567–569.

[5]Lee, T. W., "Vibration Frequencies for a Uniform Beam with One End Spring-Hinged and Carrying a Mass at the Other Free End," *Journal of Applied Mechanics*, Vol. 40, No. 3, 1973, pp. 813–815.

M. P. Nemeth
Associate Editor

Fiber-Optic Sensors for the Study of Spacecraft-Thruster Interactions: Ion Sputtering

Andrew D. Ketsdever*
U.S. Air Force Research Laboratory, Edwards Air Force Base, California 93524
and
Brian M. Eccles†
University of Southern California, Los Angeles, California 90089-1191

Introduction

THE interaction between thruster effluents and spacecraft surfaces has received considerable attention recently. Historically, thruster interaction concerns have focused on self-contamination from nondirect and high-angle (measured from the thruster centerline) plume impingement. The growing popularity of distributed networks of cooperative, coorbiting satellite clusters has brought about an additional need to address direct plume impingement or cross contamination. Typically, quartz crystal microbalances (QCMs) are used to investigate spacecraft-thruster interactions where the major contamination mechanism is the adsorption of molecular species on critical surfaces.[1] New methods are required to investigate the complex nature of plume impingement from advanced ion electric thrusters where the major interaction is the sputtering of critical surfaces. Additionally, QCMs are limited in that they only provide interaction data at a single point; however, the plume characteristics of a typical ion thruster can vary by several orders of magnitude over short distances. This study focuses on the proof-of-principle demonstration of a fiber-optic contamination sensor (FOCS), which can provide a complete interaction map for ion thrusters as an alternative to QCMs. The FOCS measures the depletion of light transmitted through the fiber as the cladding material is removed (sputtered) by energetic plume ions. Although this work is primarily concerned with assessing the FOCS for highly energetic ion interactions that induce material sputtering, the sensor might also be appropriate as an adsorption monitor for molecular contaminants.[2]

Presented as Paper 2001-2958 at the 35th Thermophysics Conference, Anaheim, CA, 11–14 June 2001; received 2 July 2001; revision received 29 August 2001; accepted for publication 30 August 2001.

*Senior Research Engineer, Propulsion Directorate, Aerophysics Branch. Senior Member AIAA.

†Undergraduate Student, Department of Aerospace and Mechanical Engineering. Student Member AIAA.

FOCS Principle of Operation

The difference in the index of refraction between the core and cladding is responsible for propagating the light signal through the optical fiber. Although the light traveling in the fiber can be thought of as undergoing total internal reflection at the core-cladding boundary, a fraction of the light, referred to as the evanescent wave, actually penetrates into the cladding before being reflected back into the core.[3] The characteristic penetration length of the evanescent wave is defined as the distance at which the intensity drops to e^{-1} of its initial intensity (at the core-cladding boundary) and is given by

$$\beta^{-1} = (\lambda/2n_{\text{clad}})\left(n_{\text{core}}^2 - n_{\text{clad}}^2\right)^{-\frac{1}{2}} \tag{1}$$

where λ is the transmitted wavelength and n_{core} and n_{clad} are the indices of refraction for the core and cladding material, respectively. The intensity of the evanescent wave decreases exponentially with increased distance from the core-cladding interface. If the core is sufficiently eccentric, the tail of the evanescent wave extends beyond the cladding into the surrounding environment. This condition is representative of light propagation through the sputtered (or etched) cladding of an optical fiber, where the thickness on one side of the core has been significantly reduced. As the sputtering process continues, more of the evanescent tail would be exposed to the sensor environment, causing a decrease in the transmitted signal strength. The rate of decrease would be proportional to the sputter rate and could conceivably be calibrated to allow for the estimation of energetic ion flux at the sensor location.

Experimental Setup: Simulated Ion Sputtering

To simulate the effects of xenon ion sputtering on optical fiber, the fiber was etched in an acid solution. Hydrofluoric acid (HF) was used, because of its strong reaction with silicon dioxide. The primary goal of this experiment was to observe the decrease in transmitted light level as a function of the optical fiber cladding thickness during the etching. Corning® SMF-28™ single-mode fiber was used, which consisted of a 8.2-μm-diam doped SiO_2 core, a 125-μm-diam pure SiO_2 cladding, and a 245-μm-diam acrylate protective coating. For light with a wavelength of 1550 nm, n_{core} and n_{clad} are 1.4505 and 1.4447, respectively.[4] The 245-μm acrylate coating was removed from a 5-cm segment of the fiber using an acetone bath, exposing the cladding for HF_{aq} etching. The light signal was provided by a 1.6-mW, fiber-coupled diode laser, which was determined to have an operating wavelength of 1304 nm. A gallium-arsenide infrared detector was coupled at the other end of the fiber to monitor the output signal. The exposed section of the fiber cladding was immersed in the HF_{aq} while the transmitted intensity was monitored as a function of time. The acid etched the circumference of the fiber evenly from all directions, which is physically different from energetic ion sputtering on only the surface facing the incident thruster plume. However, the results yielded proof-of-principle demonstration for the FOCS operation.

Results

Figure 1 shows the laser light intensity as a function of time (i.e., cladding thickness) for optical fibers in 49 and 20% HF_{aq} solutions (by weight). The etch rate for the 49% HF_{aq} was estimated to be 1.6 μm/min, which is similar to published results for silica.[5] The etch rate for the 20% HF_{aq} was estimated to be 0.16 μm/min. In Fig. 1 the intensity remains relatively constant until the fibers are etched to a diameter of approximately 21.3 μm. This corresponds to a remaining cladding thickness of 6.55 μm or 5λ. From Eq. (2) the characteristic length of penetration β^{-1} of the laser light into the cladding material is approximately 3.5 μm or 2.7λ. As expected, the transmitted signal does not degrade until the cladding thickness approaches β^{-1}. The noise seen in the traces is most likely caused by the fast etch rate, which is known to leave a rough surface.[5] The repeatability of the data in Fig. 2 suggests that a fiber sensor used to investigate sputter removal of cladding material can be adequately calibrated. To make the experimental results meaningful for spacecraft contamination studies, it is necessary to correlate the measured HF_{aq} etch rate to an estimated ion sputter rate for some thruster.

Estimated Sputtering Rates for Hall Thrusters

The SPT-100 Hall thruster is used in this study as a benchmark thruster because adequate experimental results for the thruster plume are reported in the literature. The sputter rate for SiO_2 impacted by the energetic plume of an SPT-100 has been obtained from two sources. First, Randolph et al.[6] experimentally measured the sputter rate for a quartz engineering surface 1 m downstream of the SPT-100 at various angles relative to the thruster centerline. Second, theoretical results for the sputter yield were obtained by the transport-of-ions-in-matter (TRIM) computational model, which utilizes a Monte Carlo numerical approach with a fully quantum mechanical treatment of ion-atom collisions.[7] The TRIM-derived sputter yields were then combined with SPT-100 plume characteristics experimentally obtained by King and Gallimore[8] in order to estimate an ion sputter rate. The sputter rate at a given point in the plume for a material impacted by an energetic ion beam is given by

$$\frac{\mathrm{d}x}{\mathrm{d}t} = \frac{\Phi(x,\phi)\bar{\gamma}(E,\theta)}{\rho}, \qquad \bar{\gamma}(E) = \frac{\int_0^\infty f(E)\gamma(E)\,\mathrm{d}E}{\int_0^\infty f(E)\,\mathrm{d}E} \tag{2}$$

where $\Phi(x,\phi)$ is the ion flux from the thruster at some axial (x) and radial (ϕ) location downstream of the exit plane (ions/cm^2 s); $\bar{\gamma}(E,\theta)$ is the average sputter yield as a function of ion impact energy (E) and incident angle (θ); ρ is the number density of the sputtered material (atoms/cm^3); and $f(E)$ is the ion energy

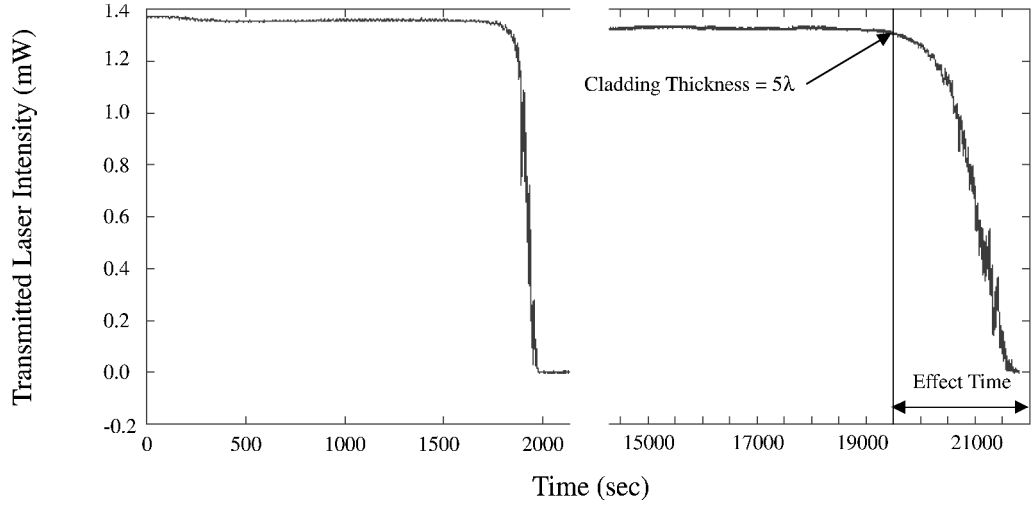

Fig. 1 Transmitted laser intensity as a function of time during 49% (left) and 20% (right) HF_{aq} etch of SiO_2 optical fiber cladding.

distribution function at a given axial and radial position in the plume.

Discussion: Sensor Utility

Table 1 gives the sputter rates for a SiO_2 material surface impacted 1 m downstream of an SPT-100, as determined both experimentally and numerically. The effect time is defined as the time required to remove the final 5λ of cladding thickness, as shown in Fig. 2 (i.e., the time needed to go from maximum to zero signal transmission through the optical fiber). The experimental results were obtained for a quartz surface oriented such that the ions were normally incident or $\theta = 90$ deg. The numerical results were calculated assuming that the incidence angle of the ions impacting the SiO_2 surface was equal to the divergence angle from the thruster centerline or $\theta = \phi$. For normally incident ions the sputter rate is driven by the decrease in ion flux as the plume angle increases because the sputter yield can be considered constant for a given energy. However, the numerical results show that when the sputtered surface is held perpendicular to the thruster centerline, such that $\theta = \phi$, the sputter rate does not drop off as quickly for higher divergence angles because of the increased sputter yield at the corresponding higher incident angles counteracting the decrease in energetic ion flux. As shown in Table 1, the predicted effect time can vary greatly depending on the incident angle of the ions on the SiO_2 surface.

Table 1 Estimated sputter rates and corresponding effect times for FOCS 1 m downstream of an SPT-100 Hall thruster

	$\theta = 90$ deg		$\theta = \phi$	
ϕ, deg	dx/dt[6], μm/min	Effect time, h	dx/dt, μm/min	Effect time, h
0	——	——	1.68E−02	6.5
15	1.03E−02	10.6	——	——
30	2.00E−03	54.3	8.55E−04	127.1
45	6.18E−04	175.8	——	——
60	6.06E−05	1,793.2	8.28E−04	131.2
80	6.90E−06	15,749	5.52E−04	196.9

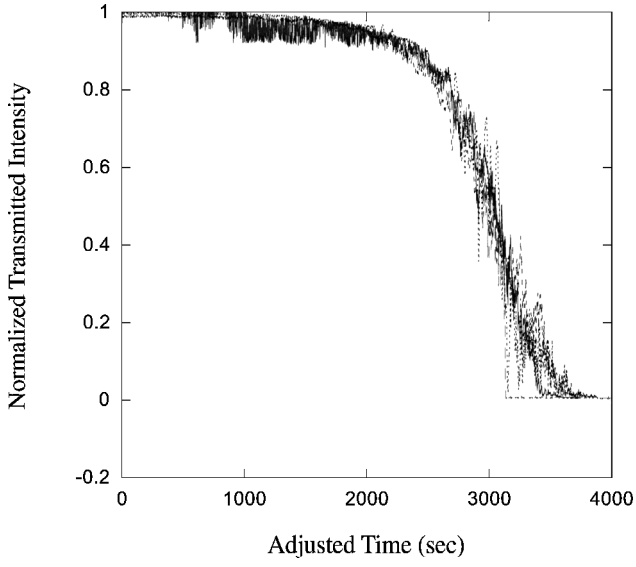

Fig. 2 Transmitted laser intensity as a function of time during 20% HF_{aq} etch of SiO_2 optical fiber cladding. Repeatability of etch results is shown for four separate optical fibers.

A potential configuration for FOCS monitoring of on-orbit spacecraft interactions can be envisioned as a two-dimensional grid of optical fibers installed on a critical surface such as a solar array panel. As a sensor system, multiple fibers can be connected to a single-diode laser source and detector with coupling to allow independent measurement of a given fiber. At various locations of interest on the FOCS grid, the fiber cladding would be exposed to the spacecraft environment. Also, the amount of cladding removed prior to installation could be varied at different locations, which would allow contamination measurement in different phases of the spacecraft lifetime. This arrangement of sensors would allow the gathering of contamination data from the FOCS locations on the grid, thereby providing a more complete understanding of the spatial and temporal thruster interaction.

Conclusions

The FOCS principle of operation has been verified in a proof-of-principle demonstration. A decrease in transmitted signal strength was observed as the optical fiber cladding thickness decreased during the HF_{aq} solution etch. The experimental results obtained in this study simulated the sputtering of optical fiber cladding material by energetic ions in the plume of ion electric thrusters. The repeatability of the HF_{aq} etch results indicate that the sensor can be calibrated for transmitted light intensity as a function of cladding thickness. Measured and calculated sputter rates for a SPT-100 plume impacting a SiO_2 surface were used to calculate values for the FOCS effect time based on correlations with the measured HF_{aq} etch characteristics. Results indicate that the transmitted light intensity will go from maximum to zero signal in approximately 6.5 h if the sensor is placed 1 m downstream of an SPT-100 on the thruster centerline. This effect time is shown to increase as the divergence angle from the thruster centerline increases. Placing the optical fiber perpendicular to the thruster centerline can reduce the predicted effect time at high plume angles. In the perpendicular configuration effect times less than one-tenth of the design lifetime of a typical Hall thruster ($\sim$2000 h) can be achieved for almost any plume angle.

References

[1]Spanjers, G., Schilling, J., Engelman, S., Bromaghim, D., and Johnson, L., "Preliminary Analysis of Contamination Measurements from the ESEX 26 kW Ammonia Arcjet Flight Experiment," AIAA Paper 1999-2709, June 1999.

[2]Ketsdever, A., Eccles, B., Abid, M., Netherwood, G., and Fitzpatrick, C., "Fiber Optic Sensors for the Study of Spacecraft-Thruster Interactions: Ion Sputtering," AIAA Paper 2001-2958, June 2001.

[3]Hecht, J., *Understanding Fiber Optics*, 3rd ed., Prentice–Hall, Upper Saddle River, NJ, 1999, p. 64.

[4]Corning, Inc., "Corning SMF-28 Optical Fiber: Product Information," PI1036, Corning, NY, April 2001.

[5]Williams, K., and Muller, R., "Etch Rates for Micromachining Processing," *Journal of Microelectromechanical Systems*, Vol. 5, No. 4, 1996, pp. 256–269.

[6]Randolph, T., Pencil, E., and Manzella, D., "Far-Field Plume Contamination and Sputtering of the Stationary Plasma Thruster," AIAA Paper 94-2855, June 1994.

[7]Ziegler, J., Biersack, J., and Littmark, U., *The Stopping and Range of Ions in Solids*, Pergamon, New York, 1985, p. 202.

[8]King, L., and Gallimore, A., "Ion Energy Diagnostics in the Plume of an SPT-100 from Thrust Axis to Backflow Region," AIAA Paper 98-3641, July 1998.

I. D. Boyd
Associate Editor